Distribution Agreement

In presenting this thesis as a partial fulfillment of the requirements for a degree from Emory University, I hereby grant to Emory University and its agents the non-exclusive license to archive, make accessible, and display my thesis in whole or in part in all forms of media, now or hereafter now, including display on the World Wide Web. I understand that I may select some access restrictions as part of the online submission of this thesis. I retain all ownership rights to the copyright of the thesis. I also retain the right to use in future works (such as articles or books) all or part of this thesis.

Nadine Juwita Jacquez April 16, 2014

Mapping the major connections of the amygdala in chimpanzees and humans using diffusion tensor imaging (DTI) and probabilistic tractography

by

Nadine Juwita Jacquez

Dr. Todd M. Preuss
Adviser

Neuroscience and Behavioral Biology Program

Dr. Todd M. Preuss

Adviser

Dr. James K. Rilling

Committee Member

Dr. Dietrich W. Stout

Committee Member

2014

Mapping the major connections of the amygdala in chimpanzees and humans using diffusion tensor imaging (DTI) and probabilistic tractography

By

Nadine Juwita Jacquez

Dr. Todd M. Preuss

Adviser

An abstract of
a thesis submitted to the Faculty of Emory College of Arts and Sciences
of Emory University in partial fulfillment
of the requirements of the degree of
Bachelor of Sciences with Honors

Neuroscience and Behavioral Biology

2014

Abstract

Mapping the major connections of the amygdala in chimpanzees and humans using diffusion tensor imaging (DTI) and probabilistic tractography

By Nadine Juwita Jacquez

The amygdala plays a key role in emotional processing and social behaviors in humans, nonhuman primates, and other mammals. Although it is well established that the mammalian amygdala can be divided into three anatomically and functionally distinct subregions – basolateral, centromedial, and cortical – the internal organization of these divisions and the absolute and relative sizes of their connections vary substantially across species. Despite this, studies of connectivity of the amygdala have heretofore been concentrated in a relatively few experimental species – mainly rodents and macaque monkeys. The development of the noninvasive diffusion tensor imaging (DTI) technology has made it possible to extend studies of connectivity to humans, and in this study, to chimpanzees, our closest relatives. It gives us an opportunity to compare humans to chimpanzees (and to macaques, based on the literature), and gain insight into how the organization of the amygdala changed during human evolution. In this study, DTI and probabilistic tractography were used in a study of the distribution of the major connections of the amygdala in chimpanzees and humans. From this, we expected to identify the three major subregions in both species and compared their size and distribution in humans to interrogate possible differences in amygdalar organization between species. My hypothesis was that the basolateral subdivision tracts would be proportionately larger and stronger in humans as compared to chimpanzees, because of its strong connections to sensory and association areas, and the dramatic increase in

the amount of association cortex in human evolution. Furthermore, I hypothesized that the centromedial and the cortical division tracts in humans would be proportionately smaller because of their strong connections to brainstem regions, and primary olfactory cortex, respectively.

Mapping the major connections of the amygdala in chimpanzees and humans using diffusion tensor imaging (DTI) and probabilistic tractography

By

Nadine Juwita Jacquez

Dr. Todd M. Preuss

Adviser

A thesis submitted to the Faculty of Emory College of Arts and Sciences
of Emory University in partial fulfillment
of the requirements of the degree of
Bachelor of Sciences with Honors

Neuroscience and Behavioral Biology

2014

Acknowledgements

First and foremost, I sincerely thank Dr. Todd Preuss for allowing me to conduct research in his lab and providing me with invaluable mentorship throughout my research experiences. I am grateful to Katherine Bryant for her mentorship, discussions and hours spent on helping me with data acquisition and trouble shooting. I wholeheartedly appreciate the individualized mentorship and support that both these mentors provided me with over the past three years and value the lessons they have imparted onto me.

I also thank Dr. Longchuan Li for help with FSL instruction and registration methods, Dr. James Rilling and Dr. Dietrich Stout for guidance and feedback as committee members, and Mary Ann Cree for her administrative and personal support. Lastly, I would like to thank and acknowledge my father, Anthony, for the sacrifices he has made and the unconditional support has for me, so that I could pursue my scientific passion at Emory University.

Table of Contents

1. Introduction

The amygdala is a complex brain structure that is involved in a wide range of normal behavioral functions and psychiatric conditions, particularly those implicated in social behavior and emotional processing. It is an almond-shaped mass of nuclei that is nestled in the anteromedial temporal lobe of the brain. The amygdalar region does not exist as a single unit, but is rather a collection of nuclei generally agreed to be grouped under three main subdivisions conventionally called the basolateral amygdala (BLA), centromedial amygdala (CEA), consisting of the central and medial nuclei, and cortical amygdala (CA). These subdivisions are both anatomically and functionally distinct. For example, both the basolateral and centromedial nuclei are involved in mediating positive and negative reward in order to influence behavior. Particularly, the BLA has been implicated in adding valence to stimuli, encoding a predictive relationship between environmental stimuli and affect (Murray, 2007). This is thought be due to its strong connections to the orbitofrontal region (Baxter and Murray, 2002). Conversely, the central amygdala is thought to use this value-associated information from the BLA and mediate a behavioral response in the individual, particularly through its connectivity with lower brain regions such as the periaqueductal gray, hypothalamus, basal forebrain and the brainstem. In fact, the central amygdala is the sole amygdalar input to the PAG and this connection generates behavioral freezing, the most common variable measured in fear conditioning (LeDoux et al., 1988). But more generally, the PAG is connected with autonomic nuclei in the brainstem that generate emotional behaviors

(LeDoux et al, 1888). Moreover, the cortical amygdala is involved in olfactory associations and sexual behavior (Lehman et al., 1980). Although there exist some basic similarities across mammalian amygdala, the internal organization of these anatomically and functionally distinct divisions and their absolute and relative sizes may vary substantially across species (Pabba, 2013). Standard functional and structural magnetic resonance imaging alone (MRI) can typically only analyze the amygdala as a whole, and does not allow for the analysis of its individual subregions (Saygin, 2011). With diffusion tensor imaging (DTI), one can distinguish between structures not seen in structural MRI, as well as visualize the direction, spatial location, and magnitude of white matter tracts (Assaf, 2007). Because of this, DTI potentially allows for identification of individual, homologous subregions across species. Although previous studies have attempted to segment the human amygdala using connectivity patterns from (DTI) and probabilistic tractography (Saygin, 2011), there have been no comparable published chimpanzee studies to date.

Diffusion tensor imaging and probabilistic tractography offer new ways of mapping the brain noninvasively, *in vivo*. DTI depends on the principle of "Brownian motion", or random movement of particles that is caused by thermal energy (Le Bihan, 2001). DTI relies on the ability of water to move along myelinated axons with a high propensity (Saygin et al, 2011). This is due to fact that water molecules can move more easily through axons because they are typically free of obstacles such as cellular membranes and other structural barriers, and thus have the freedom to diffuse with a directional bias or

anisotropic diffusion, so as to lead to faster synaptic communication (Ciccarell et al, 2006). With DTI, diffusion anisotropy can be identified, characterized and used for fiber tracking (Le Bihan, 2001). Higher anisotropy is indicative of more cohesive fiber bundles and higher myelin content, as in white matter, while lower anisotropy is indicative of grey matter. characterized by lower myelin content and greater numbers of crossing fibers (Le Bihan, 2001). When trying to assess brain connectivity using DTI, one can use statistical probability to infer continuity of fiber orientation from voxel to voxel (Le Bihan, 2001). Using probabilistic tractography, fiber tracts can be reconstructed based on calculations of a voxel-based connectivity index (Ciccarell et al, 2006).

It is clear that there are behavioral differences between the emotional and social processing of information in even our closest relative, the chimpanzee, and humans. Previous studies have investigated the neurobiological basis behind these important behavioral differences in chimpanzees and bonobos, particularly the comparative connectivity of the amygdala and its impact on social cognition (Rilling et al., 2011). In order to investigate how the human brain, particularly the amygdala, was modified in human evolution, I have delineated the subregions of the amygdala of chimpanzee and humans and compared the size of the tracts and distribution of the amygdalar subregions. The purpose of this study is to investigate functional and neuroanatomical evolution in the human lineage. In order to answer the question of what brain features make human beings unique, I will compare the differences in the strength of connectivity between the amygdala and various parts of the brain that have been shown to have specific connections

to particular subnuclei in the amygdala, as well as the different sizes and spatial distributions of the amygdala subdivisions using known connections.

In order to parcellate the amygdala in chimpanzees and humans, methods based on cortical connectivity utilizing DTI and probabilistic tractography were used by drawing masks of regions of interest (ROIs) on the amygdala and on target structures with specific connectivity to the amygdala subregions on T1-weighted images. These regions were chosen based upon a literature survey of histological and tracer neuroanatomical studies. These seed regions were used to localize the amygdala structures and assess their connections; these include the orbital frontal cortex and temporal cortex to the basolateral amygdala, the olfactory cortex to the cortical amygdala, and the periaqueductal gray to the centromedial amygdala (Saygin, 2011).

My hypothesis is that the humans should have more connections with structures that connect with the basolateral amygdala, specifically the cortical masks (OFC and temporal cortex). This is based on a previous study that had shown that this subdivision is larger in humans than predicted by allometry, correlating with social group size and parvocellular visual pathway size (Barton, 2000). It has also been shown that the neuronal population in the basolateral division, particularly the lateral nucleus, is larger in humans as compared to nonhuman apes in an allometric analysis (Barger, 2012). This suggests that the lateral region may be where human specialization took place within the amygdala. In addition, the basolateral division has been implicated as serving as

the evolutionarily structure that controls the older central amygdala and is responsible for more complex emotional learning (Laberge, 2006).

2. Methods

2.1. *Subjects*

Both T1-weighted and diffusion-weighted MRI (dw-MRI) scans were collected from 6 female chimpanzees (*Pan troglodytes*, 29.4 ± 12.8 yrs) and 6 female humans (*Homo sapiens*, 42.5 ± 9.8 yrs), which were selected from larger cohorts by two independent raters for highest quality scanning, such as a strong white matter/gray matter contrast and accurate skull-stripping. All chimpanzees were housed at the Yerkes National Primate Research Center (YNPRC) in Atlanta, Georgia. All procedures were carried out in accordance with protocols approved by the YNPRC and the Emory University Institutional Animal Care and Use Committee (IACUC, approval #: YER-2001206). All female human and chimpanzees participants were collected as part of a large, comparative study on brain aging. The human participants were healthy aging volunteers with no known neurological disorders (IRB approval #: IRB00000028).

2.2. *MRI acquisition*

The anatomical and diffusion MR data for both species were acquired on two Siemens 3T Trio Tim Scanners (Siemens Medical System, Malvern, PA). Chimpanzees were immobilized with ketamine (2–6 mg/kg, i.m.) before to being anesthetized with isoflurane (1%). The animals were under constant observation by the veterinary staff before, during, and after the scan. Foam cushions and

elastic straps were used to stabilize head motion. For diffusion imaging, equal sets of diffusion-weighted images with phase-encoding directions (left–right) of opposite polarity were acquired for removing susceptibility-related distortion in post-processing (Andersson et al., 2003). For chimpanzees, a standard circularly polarized (CP) birdcage coil was used due to their protruding jaw which would be too large to be fit into the standard phase-array coil designed for humans. For humans, a 12-channel phase-array coil was used. The signal-to-noise ratio of the diffusion-weighted images was similar (approximately 30) for both species. Final T1 resolution was 1 mm^3 for humans and 0.8 mm^3 for chimpanzees; dw-MRI resolution was 2 mm^3 for humans and 1.8 mm^3 for chimpanzees.

2.3. *Data preprocessing*

Anatomical and diffusion MR data were analyzed using FSL FMRIB 5.0 (http://fsl.fmrib.ox.ac.uk/fsl/ fslwiki/; Jenkinson et al. 2012). Skull-stripping (Smith, 2002), intensity bias correction (Zhang et al., 2001), noise reduction (Smith and Brady, 1997), and contrast enhancement (squaring the images to improve white-matter/gray-matter contrast) were performed on the T1-weighted images before any analysis was performed. Diffusion-weighted images were first corrected for eddy-current induced distortion across diffusion directions using linear co-registration of the diffusion-weighted images to the b0 image. Then, the susceptibility distortion was corrected based on the method by Andersson et al. (2003).

2.4. *Voxelwise analysis using probability tractography*

FSL software was used to reconstruct diffusion information for all subjects using probabilistic tractography. FSL's FDT diffusion program was set to run 10,000 streamlines for each voxel of the ROIs. These streamlines tracked through the DTI scan, voxel by voxel, based on the orientation and magnitude of the first and second diffusion directions in the current voxel and the surrounding voxels. So-called "symmetric" tracking was used in order to produce robust probabilistic tracts for the whole amygdala and regions of interest. In this method for identifying pathways between two masks, both the whole amygdala ROI and one of the subnuclei-specific ROIs (OlfCtx, OFC, PAG, hippocampus, or TempCtx), were used as seed masks. Only the tracks sent from the first mask that reach the second mask are kept, and likewise, only the tracks sent from the second mask that reach the first are kept for analysis. The probability maps resulting from both tracts are summed to create the symmetric tractogram result. Results were thresholded at .99, in other words, the top 1% of voxels in the tractogram, based on probability, were retained in the final result. This strict threshold was chosen based on previous studies and was used in order to eliminate false positives and noise, leaving us with more reliable results.

2.5. *Find-the-biggest*

With the find-the-biggest parcellation of the amygdala, maximum probability maps of binary images indicate whether any target voxel had relatively stronger

connections to one or the other seed cluster, as determined by the clustering algorithm.

2.6. Mask Drawings

All masks were drawn using FSL (http://fsl.fmrib.ox.ac.uk/fsl/ fslwiki/) and T1-weighted MRI images. T1-weighted images were chosen based on their higher spatial resolution and clearer gray/white contrast in order to more accurately identify regions-of-interest (ROIs). In order to provide an objective background for investigation, ROIs and boundaries were chosen based on connectivity findings from past histological tracer studies in macaques amygdalar subnuclei. For the amygdala, first I drew a set of ROIs based on one set of criteria, which is considered “conservative”, and Dr. Preuss drew another set, which is considered “liberal” and was extended to encompass more of the surrounding brain regions. Dr. Preuss also draw the primary olfactory cortex, and the temporal cortex masks were generated using FreeSurfer’s segmentation and parcellation functions (Reuter et al., 2012), with slight modifications for use in the chimpanzee dataset. The hippocampal masks were drawn by Nicole Taylor, MS, a graduate student in Dr. Preuss's lab. The orbital frontal cortex (OFC) and periaqueductal gray (PAG) were drawn by me using FSL software.

2.6.1. *Amygdala*

I used FSL to perform the manual tracing of my regions-of-interest. In order to draw the whole amygdala mask, I adapted the procedure developed by Entis et al. (2012) in humans, which utilizes white and gray matter landmarks, and sulcal features, to estimate the borders of the amygdala. Because of the close proximity of the primary olfactory cortex to the amygdala, and because it is strongly connected with the cortical division of the amygdala, primary olfactory cortex masks were first drawn for each subject by Dr. Preuss, to ensure that the amygdala masks did not extend into the olfactory cortex. In order to accurately draw the amygdala mask, borders were drawn using both a parasagittal view and a coronal view in order to see the appropriate landmarks. The posterior edge of the amygdala was assigned by tracing the alveus, seen as a white matter band separating the amygdala from the hippocampus in the parasagittal view. The inferior border of the amygdala was drawn in the coronal plane and was identified by locating the unambiguous grey matter in the medial temporal lobe above the temporal horn of the lateral ventricle. The lateral border was defined as being the medium grey band bordering the grey matter of the claustrum. The upper margin of the entorhinal sulcus guided the drawing of the superior border of the amygdala, separating it from the putamen. Moving posteriorly, the top margin of the optic tract was used to assign the dorsal border.

After identifying these points, the next step was to draw the anterior and medial borders using the two masks drawn previously as guides. The band of white matter that underlies the entorhinal cortex was used to delineate the border

between the entorhinal cortex and amygdala. As I moved more posterior, the sulcus semilunaris—a shallow groove on the medial edge of the amygdala that separates the amygdala from the entorhinal cortex, and the hippocampus more posteriorly—was used as a landmark for the lateral border in places that were not previously defined by the previous maps. After location of the amygdala borders using the protocol above, the masks were put together to form one coherent amygdala mask and filled.

An alternative set of amygdala masks, referred to as the “liberal” amygdala mask, was drawn for each species by Dr. Preuss. This was intended to result in larger masks that include more of the peripheral portions of the amygdala, including specifically the more superior portions, which include parts of the central and medial nuclei. These are difficult to segment from adjacent gray matter structures, including the putamen and claustrum, laterally, and the basal forebrain, medially, because those structures are not always separated from the amygdala by distinct bands of white matter. Using the criteria described above as a starting point, the alternative masks were dilated dorsally by approximately 1-3 voxels to include more of the gray matter in the watershed region between the amgydala and its neighbors.

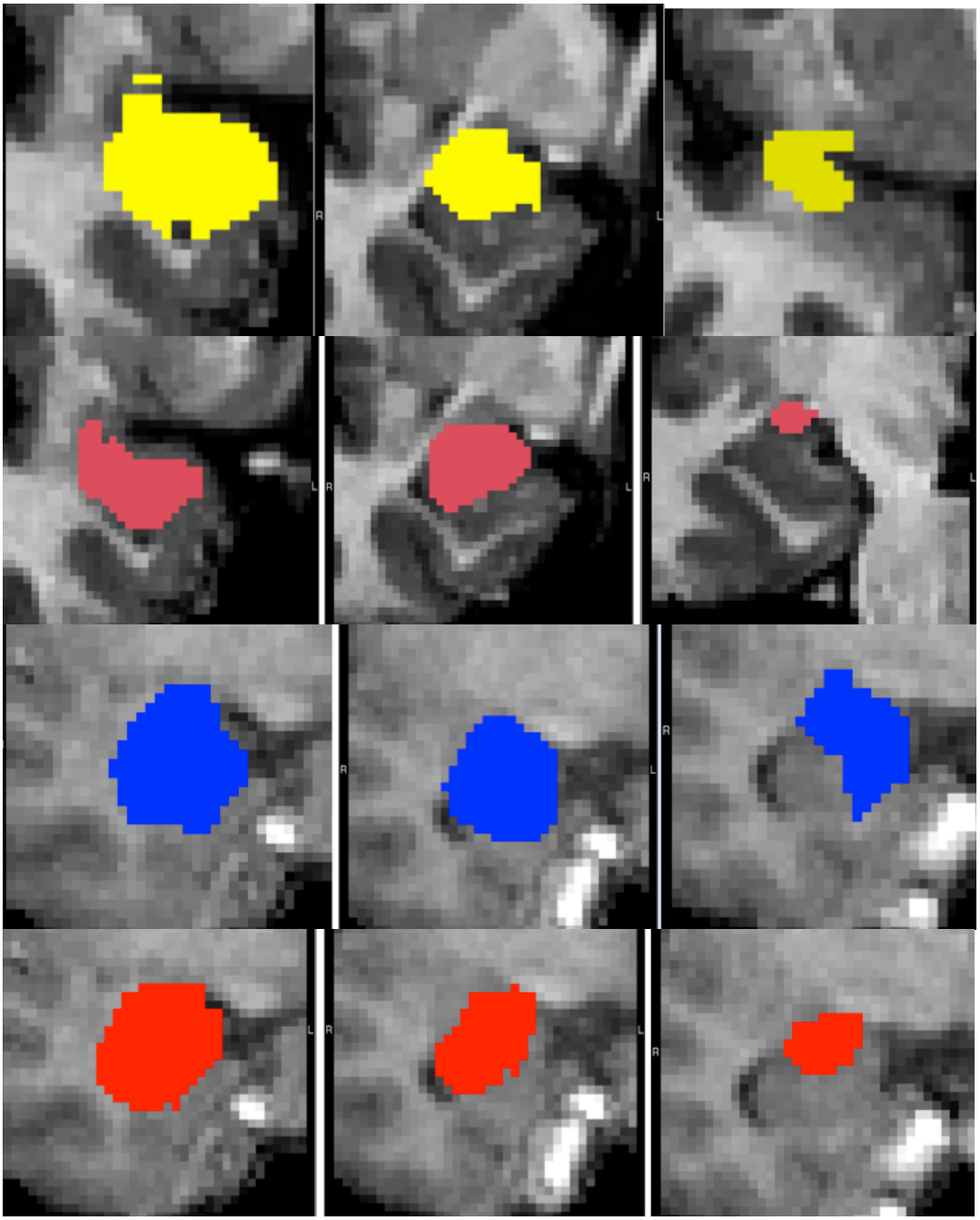

Figure 1. Amygdala mask drawings for the human and chimpanzee
The human liberal amygdala mask is drawn in yellow, the human conservative mask is drawn in pink, the chimpanzee liberal amygdala mask is drawn in blue and the chimpanzee conservative mask is drawn in red.

As seen in fig 1., the masks for the amygdala were drawn in on the T1-structural

scan. The yellow mask represents the liberal seed mask for humans and the pink

mask represents the more conservative seed mask for humans. The blue mask represents the liberal seed mask for chimps and the red mask represents the more conservative seed mask for chimps.

2.6.2. *Periaqueductal Gray*

The periaqueductal grey (PAG) mask was drawn in the coronal plane on T1 structural MRI images using FSL software. The PAG was identified by locating the cell-dense grey-matter region surrounding the cerebral aqueduct of the midbrain. The superior colliculus was used as a dorsal border and the inferior colliculus was used as a lateral border. The rostral and caudal borders were defined by the limits of the cerebral aqueduct.

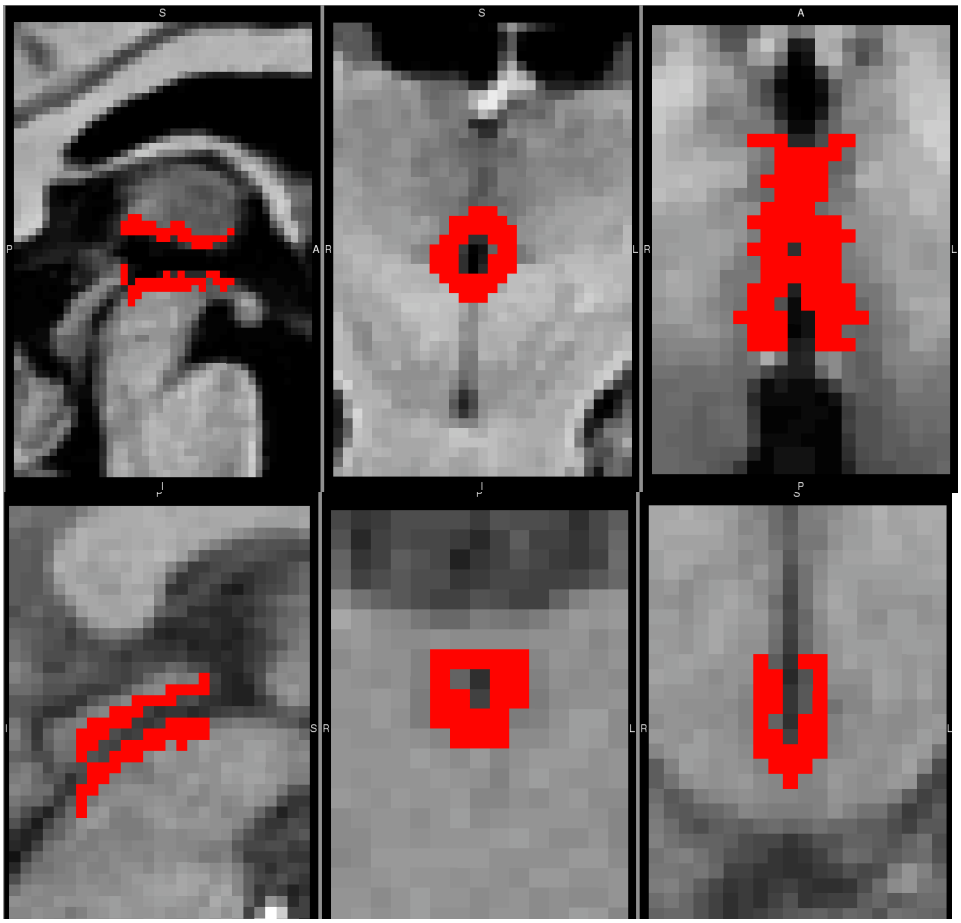

Figure 2. The PAG mask
The PAG masks (red) were drawn on T1- structural scans for humans (above) and chimpanzees (below).

2.6.3. *Olfactory Cortex*

In primates, the primary olfactory cortex is located around junction of the frontal lobe with the temporal lobe. First, the coronal section that included the most anterior point of contact between the two lobes was located. The primary olfactory cortex could be identified in T1-weighted images as a zone of relatively thick, well-myelinated (light in T1) cortex compared to its neighbors. This territory could be followed with confidence for 1-3 sections further anteriorly into the

frontal lobe, and 1-3 sections further posteriorly into the temporal lobe. To avoid including amygdala voxels in the mask, the olfactory cortex mask was restricted to its piriform division, and was not extending into its more posterior division, the periamygdaloid cortex, which lies just superficial to the anterior pole of the amygdala. In some sections, the periamygdaloid cortex can be identified as a zone of thick cortex separated from the amygdala by a fiber band, but these characteristics are not always apparent, and the border between the amygdala and periamygdaloid cortex can be difficult to locate precisely.

In order to draw the olfactory cortex mask in FSLView, the coronal view of the T1 structural MRI was used and the point at which the temporal lobe joins the base of the frontal lobe was localized as the initial plane. The mask was drawn as a thin 1-2 voxel thick extension of the cortical surface from the cortex at the base of the frontal lobe and was extended from the mediolateral middle of the putamen nucleus to where the frontal and temporal lobes join. The mask was then extended onto the adjacent surface of the temporal lobe. This extension had a medial limitation of the bulging dark matter of the amygdala, or about half the distance of the frontal lobe section of the olfactory mask. The mask was drawn thicker in this temporal section because the coronal plane is passing obliquely through the cortex. Careful precautions were taken to not include white matter into the mask, only grey matter. The olfactory cortex mask was defined anteriorly by continuing the frontal lobe cortical mask one coronal slice anteriorly. The mask was defined posteriorly by continuing the fronto-temporal cortical mask two coronal slices posteriorly, using the same medial and lateral borders defined

previously. The posterior border could also be identified by the thickening of the anterior pole of the amygdala

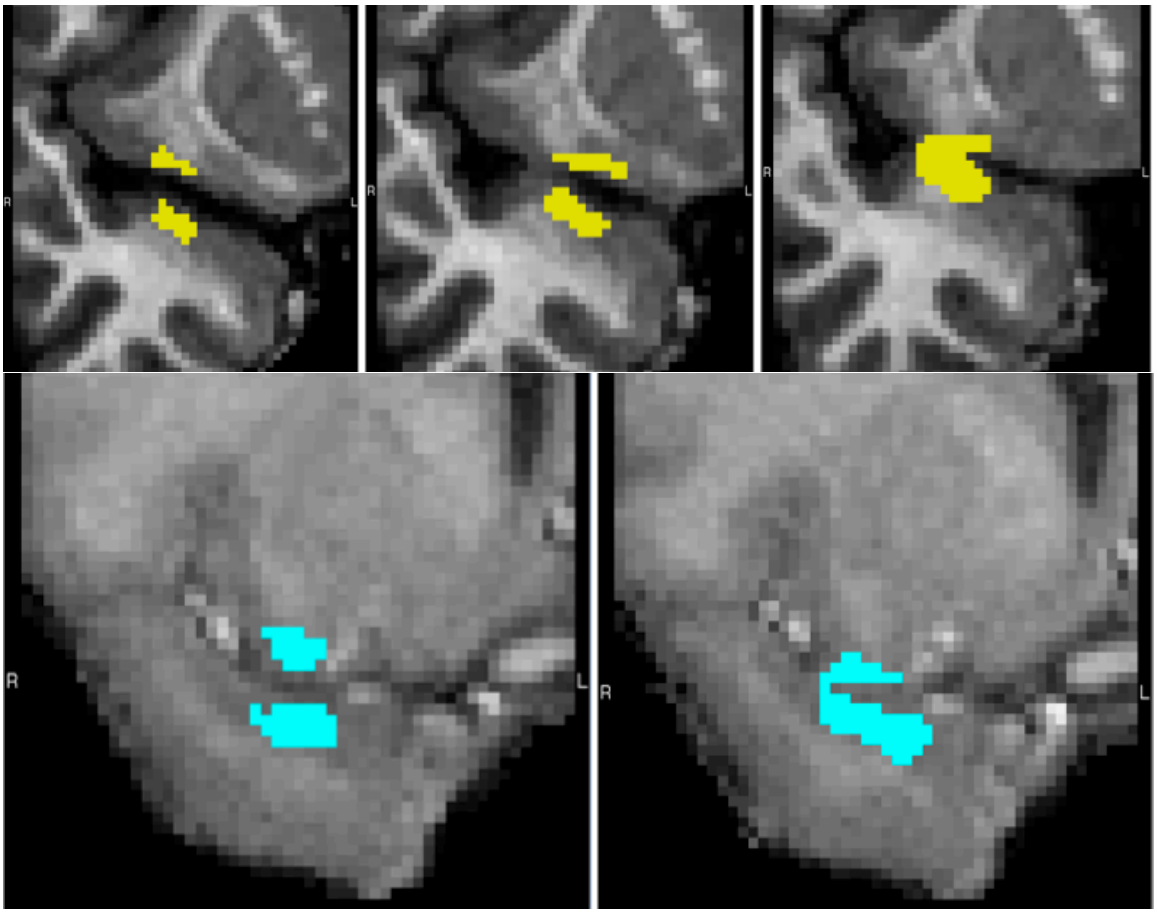

Figure 3. The olfactory cortex mask
The olfactory cortex masks were drawn on T1- structural scans for humans (yellow) and chimpanzees (blue).

2.6.4. *Orbital frontal cortex*

The OFC was drawn in the coronal plane. The cortical mask included the cortical gray matter and was extended one to two voxels into the bordering white matter. Medially, the mask was extended up to the cingulate gyrus. Laterally, the mask extended until the medial orbital sulcus in the most anterior sections of the brain and just past the posterior orbital gyrus, moving posteriorly. As soon as the

temporal pole was visible in the coronal plane of the MRI, the OFC mask was terminated posteriorly. Because the temporal lobe juts out further anteriorly in humans than it does in chimps, the chimp masks probably included more posterior orbital cortex than did the humans. The OFC masks did not extend as far posteriorly as the primary olfactory cortex. Anterior borders were established by starting the coronal plane at the most anteriorly established point as having a ventral surface, most easily seen in the parasagittal view.

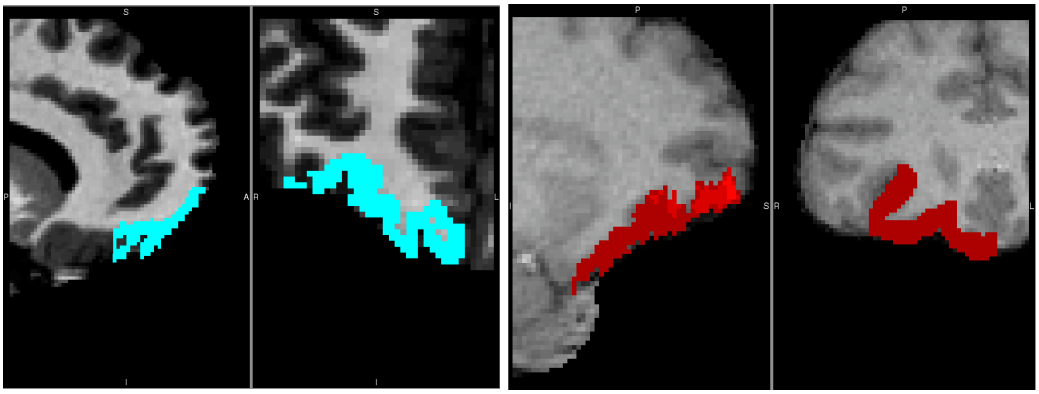

Figure 4. The OFC mask
The OFC masks were drawn on T1- structural scans for humans (blue) and chimpanzees (red).

2.6.5. *Temporal Lobe*

The temporal lobe gray matter mask was generated semi-automatically using the FreeSurfer Imaging Suite, which is documented and freely available for download online (http://surfer.nmr.mgh.harvard.edu/; for representative publications see Fischl et al. 1999, 2002, 2004). FreeSurfer's recon-all function was used on human and adjusted chimpanzee T1 scasn to perform a hard segmentation in order to isolate the cortical gray matter portion of the scans. These data were then parcellated into major gyri, converted to FSL file format,

and the gyral sections corresponding to the temporal lobe in humans and chimpanzees were identified and isolated from the rest of the gray matter to create large gray matter temporal lobe masks. Gray matter segments included in these masks included in the superior, middle, and inferior temporal gyri, the lingual gyrus, the parahippocampal cortex, the fusiform gyrus, the entorhinal cortex, and the temporal pole. The posterior limit of the temporal lobe was defined as the temporal-occipital border and the dorsal limit as the temporal-parietal border.

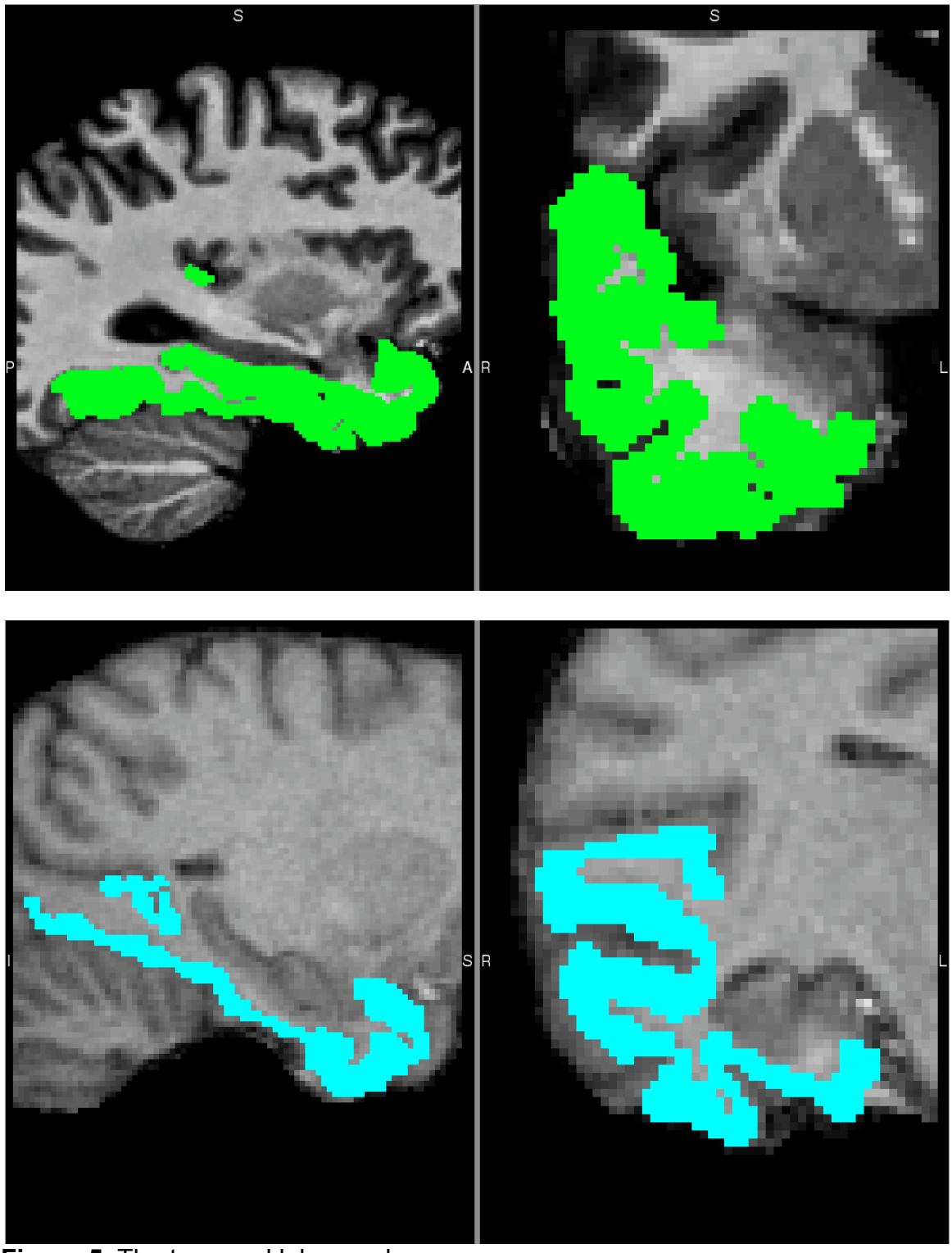

Figure 5. The temporal lobe mask
The temporal masks were generated using a semiautomatic software with humans (green) and chimpanzees (blue).

2.6.6. *Hippocampus*

In order to the draw the hippocampus, the white-matter alveus and inferior lateral ventricle were again used in the parasagittal plan to distinguish it from the amygdala. In the coronal view, the appearance of the temporal horn of the lateral ventricle was used as the starting point for the hippocampal mask. In order to define the hippocampus medially, the white matter tract that separates the hippocampus from the cortex was used and similar procedure was continued posteriorly. When the amygdala disappeared, the superior border of the hippocampus could be drawn as the border above the fimbria, characterized by thin white stripes at the dorsal end of the hippocampus. The inferior medial border followed the trajectory of the white matter tracts in the parahippocampal gyri. Moving posteriorly as the fimbria disappears, and the thalamus was used as an anatomical border. As the thalamus disappears posteriorly, the landmark borders then become the lateral ventricle laterally and white matter medially in the coronal view and this continues until the hippocampus's most posterior coronal slice.

2.7. *Quantitative Methods*

I performed several statistical analyses on amygdala connectivity using streamline counts in two mask-symmetric probabilistic tractography as a dependent variable. In order to do this, first the mask size was calculated and obtained from FSL for each non-amygdala mask for each tractography run, e.g. OFC, PAG, temporal cortex, and the olfactory cortex, and consisted of the

number of voxels making up ROI mask. Second, the thresholded tract size, the number of voxels in the thresholded tract which consisted of the top 1% of voxels in the resulting tractogram for each tractography run, was calculated and obtained using FSL. With these numbers a proportion of successful streamlines thresholded was calculated by dividing the thresholded tract size (waytotal) by the number of successful streamlines ((mask size+seed mask) x 10,000). The proportion of successful streamlines-thresholded was used to compare differences between amygdalar subdivisions within species, as well as for analysis of differences between species. All statistical analysis was performed using SPSS software.

A second analysis was conducted using the thresholded tract overlap with the amygdala as a function of the entire amygdala volume. This was done to investigate how much of the amygdala was being used to send or receive projections to and from my ROIs.

The non-parametric two-tailed Mann-Whitney U was used rather than a parametric test to compare the amygdalar subregions of chimpanzees and humans, because the proportion of successful thresholded streamlines was significantly skewed within both species (zskew > 1.96)

3. Results

3.1. *Qualitative Results*

The following tractography results are illustrated by a representative human case (Aging_Subject_02) and a representative chimpanzee case (Sylvia). Although there exist some minor differences in the individual subject's tracking

results, the spatial organization and size of tracts relatively similar across species. The coronal slices are ordered from anterior to posterior end.

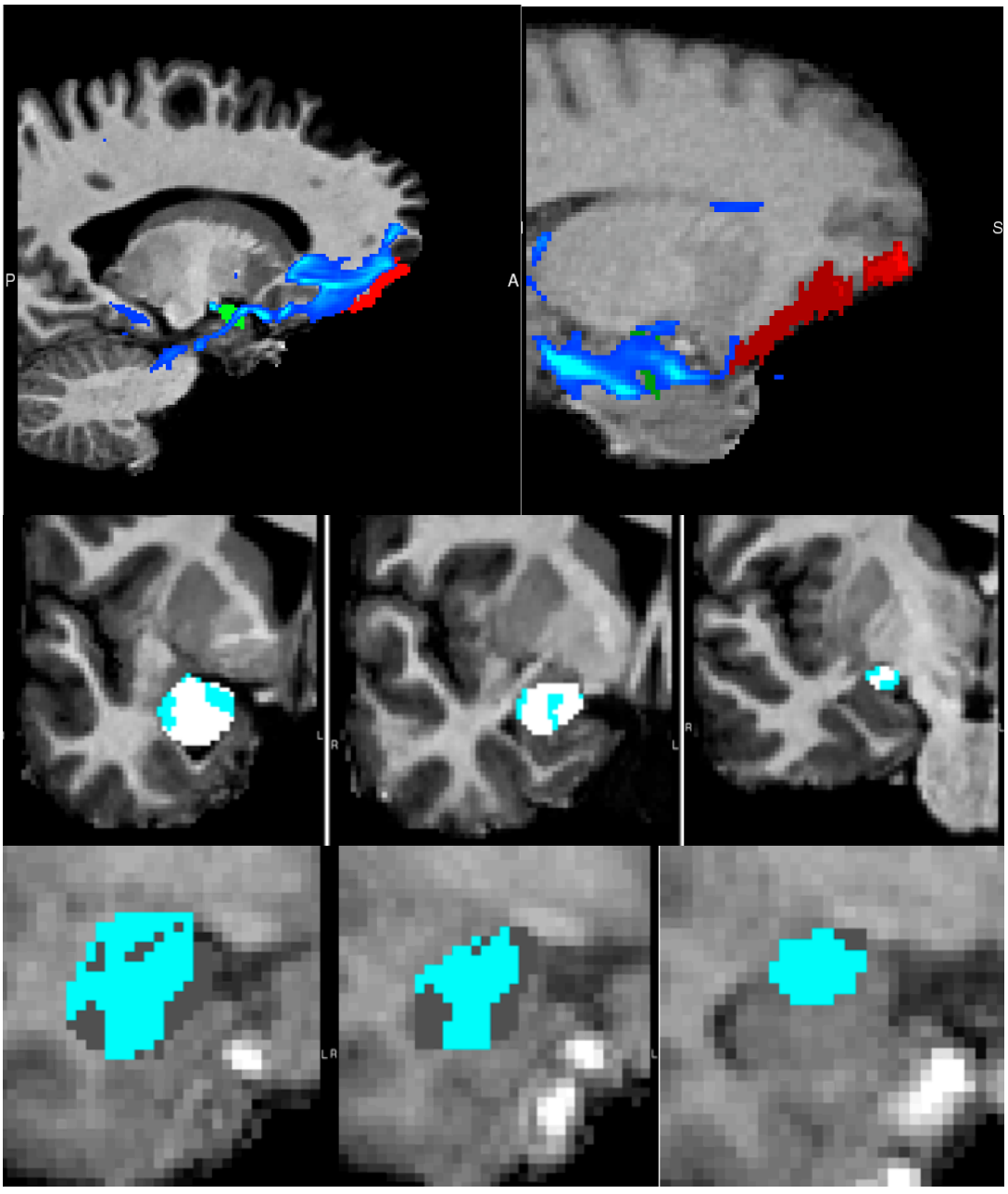

Figure 6. The OFC to amygdala tract in humans and chimpanzees. The OFC mask is represented in red, the amygdala mask is represented in green, and the thresholded tract is represented in blue, with the lighter blue indicating a higher probability of tracts. The human result is on the left and the chimp result is on the right. OFC to amygdala overlap is in light blue for both the

human (left) and chimpanzee (right). The whole amygdala mask is represented by the colored white (human) and gray (chimp) pixels.

In figure 6, we can see that the tracts related to the OFC mask ran successfully through the amygdala, and extend to the posterior and anterior regions of the amygdala in both species.

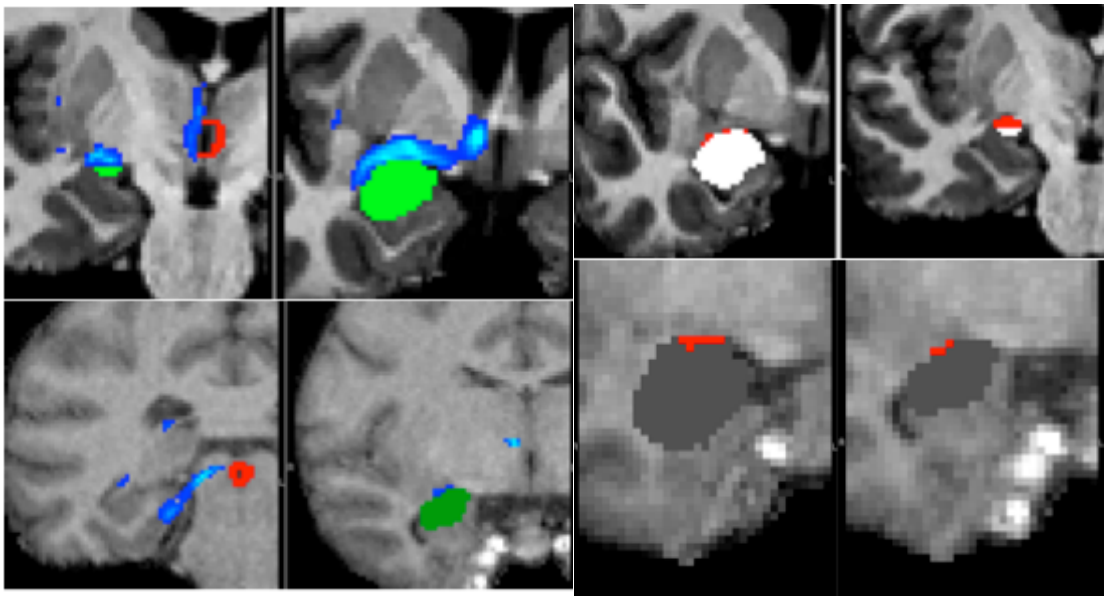

Figure 7. The PAG to amygdala tract in humans and chimpanzees.In the upper two images, the PAG mask is represented in red, the amygdala mask is represented in green, and the thresholded tract is represented in blue, with the lighter blue indicating a higher probability of tracts for the model human (above) and chimp (below). In the lower two pictures, the PAG-amygdala overlap (red) is shown for humans (above) and chimpanzees (below). The whole amygdala mask is represented by the colored white (human) and gray (chimp) pixels.

In figure 7, we see the probable connections between the PAG and the amygdala. These connections are proposed to go through the stria terminalis. From the data, this pathway looks direct, with little obstruction. It also seems to leave from the central amygdala to the medial amygdala, then to the PAG.

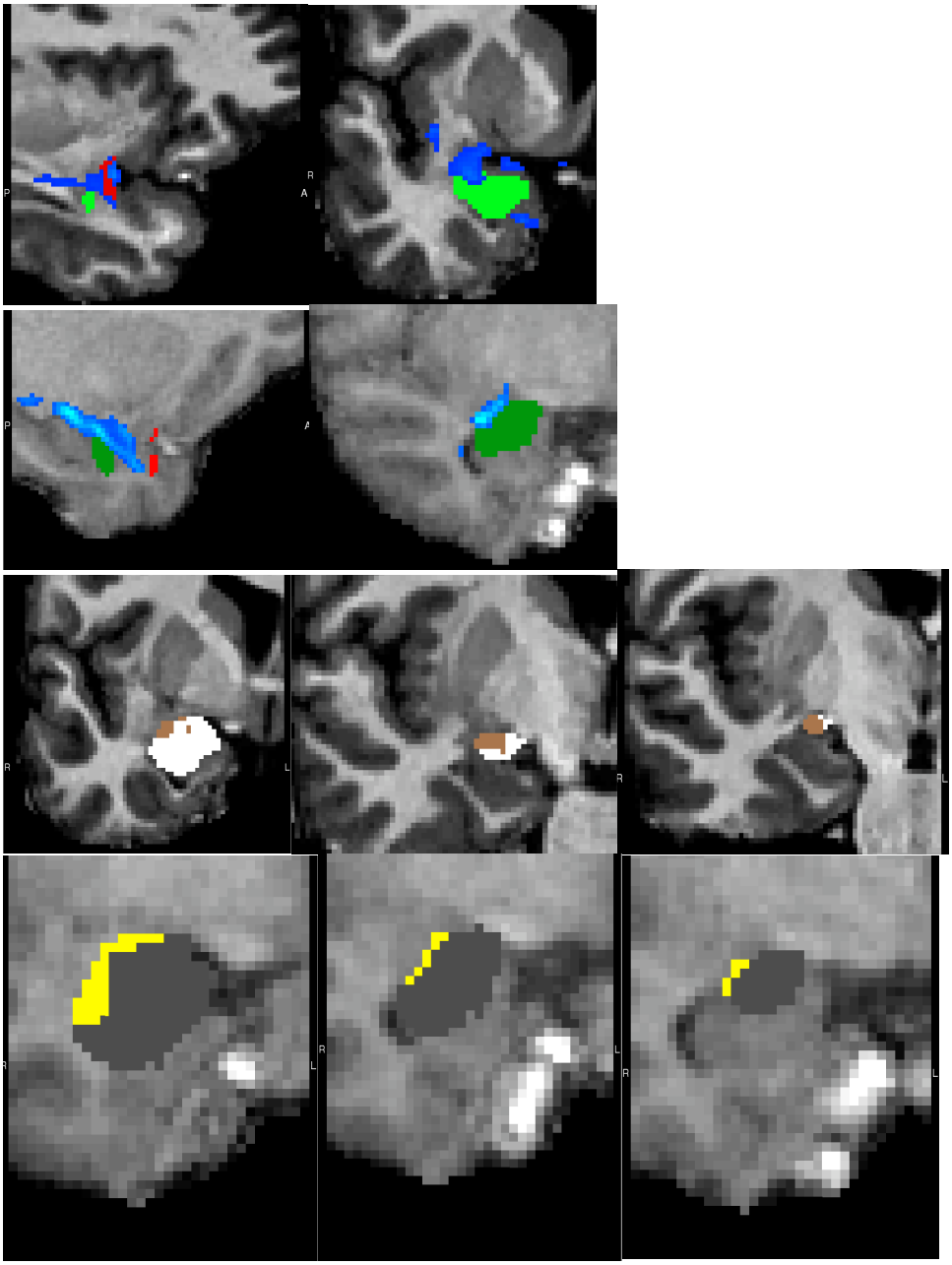

Figure 8. The olfactory cortex to amygdala tract in humans and in chimps. The olfactory cortex mask is represented in red, the amygdala mask is represented in green, and the and the thresholded tract is represented in blue, with the lighter blue indicating a higher probability of tracts (above). Olfactory cortex tract and amygdala overlap is shown in humans (brown) and chimps (yellow). The whole amygdala mask is represented by the colored white (human) and gray (chimp) pixels.

The results in figure 8 for the olfactory cortex seed show that the tracts the tracts intersected more of the cortical amygdala in chimps than in humans. However, for both species, there the tracts are located on the central amygdala and all results are localized to the superior shell of the amygdala.

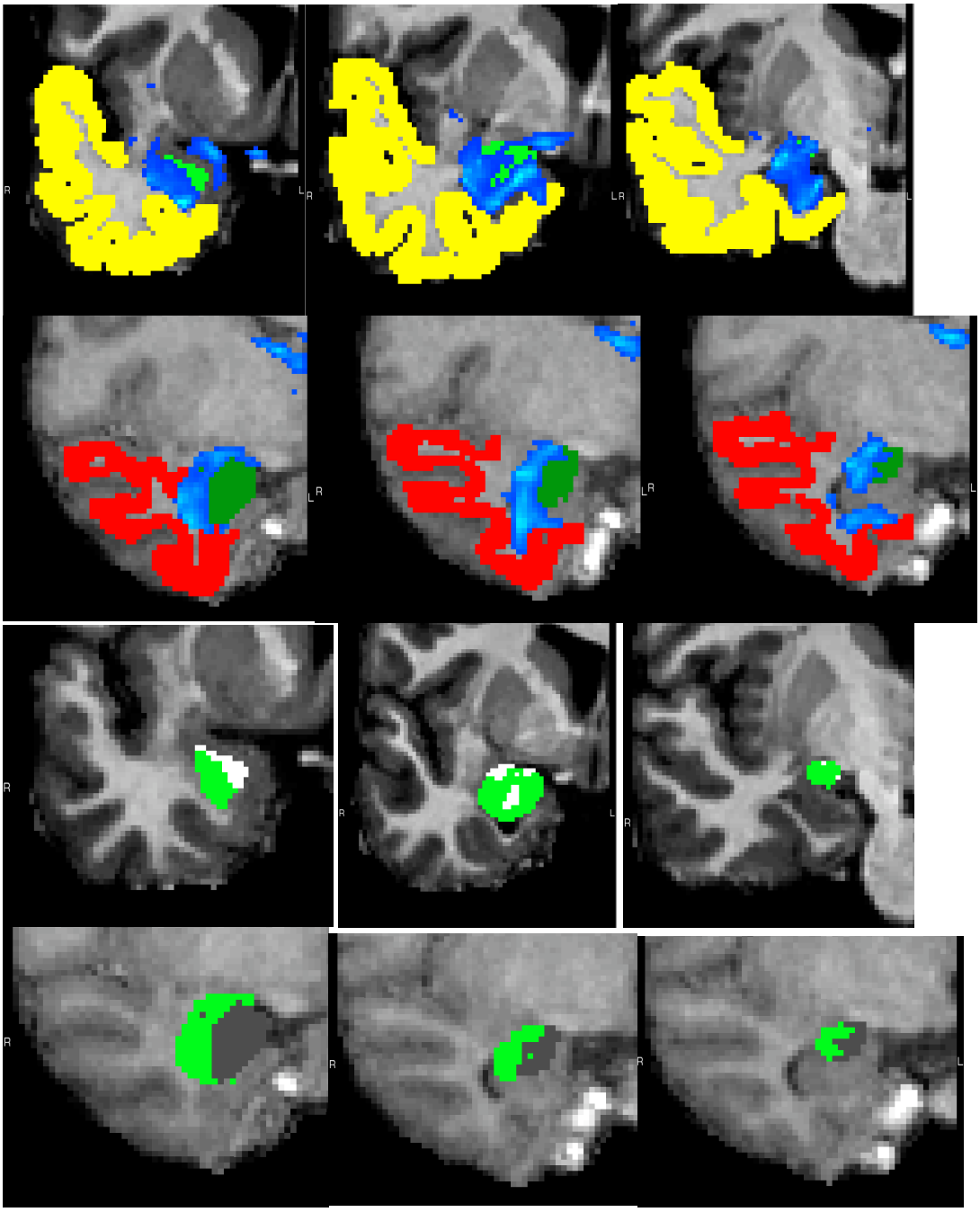

Figure 9 The temporal lobe to amygdala tract in humans and chimps
The human temporal lobe mask is represented in yellow, the chimpanzee temporal mask is represented in red, the amygdala mask is represented in green, and the and the thresholded tract is represented in blue, with the lighter blue indicating a higher probability of tracts. The overlap of the thresholded tract with the amygdala mask is shown in green. The whole amygdala mask is represented by the colored white (human) and gray (chimp) pixels.

The tracts in figure 9 show the connections between the temporal cortex and the amygdala. They seem to be localized on the medial inferior part of the temporal lobe and the lateral amygdala. The tracts extend further into the basal part of the amygdala in humans than in chimps.

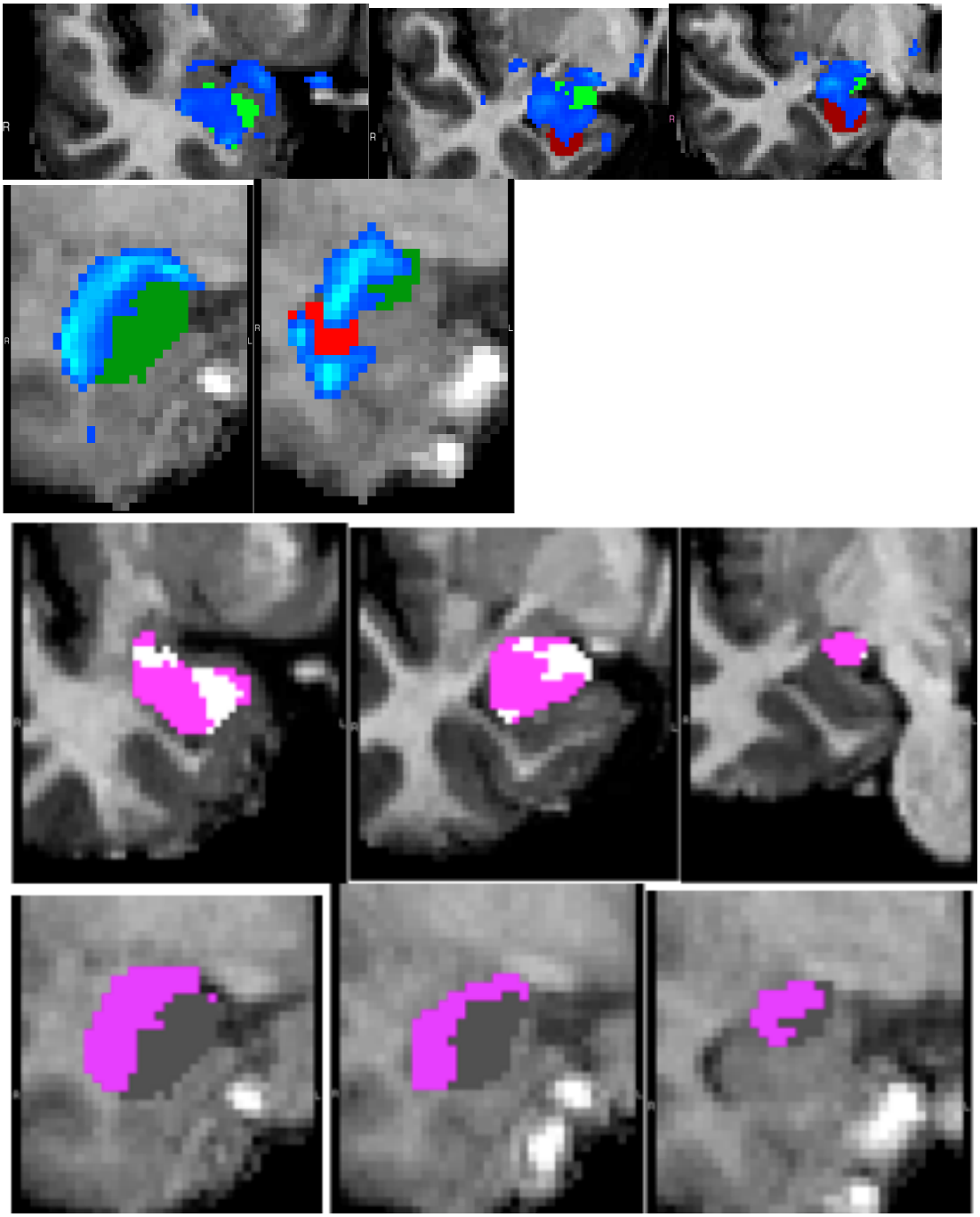

Figure 10 The hippocampus-amydgdala tracts in humans and chimps
The hippocampus mask is represented in red, the amygdala mask is represented in green, and the and the thresholded tract is represented in blue, with the lighter blue indicating a higher probability of tracts. Hippocampus-amygdala thresholded tract overlap with the amygdala mask is shown in purple. The whole amygdala mask is represented by the colored white (human) and gray (chimp) pixels.

In Figure 10, we see that the connects seem to concentrated on the centralmedial and lateral part of the amygdala in chimps and more of the basal and cortical part of the amydgala in humans.

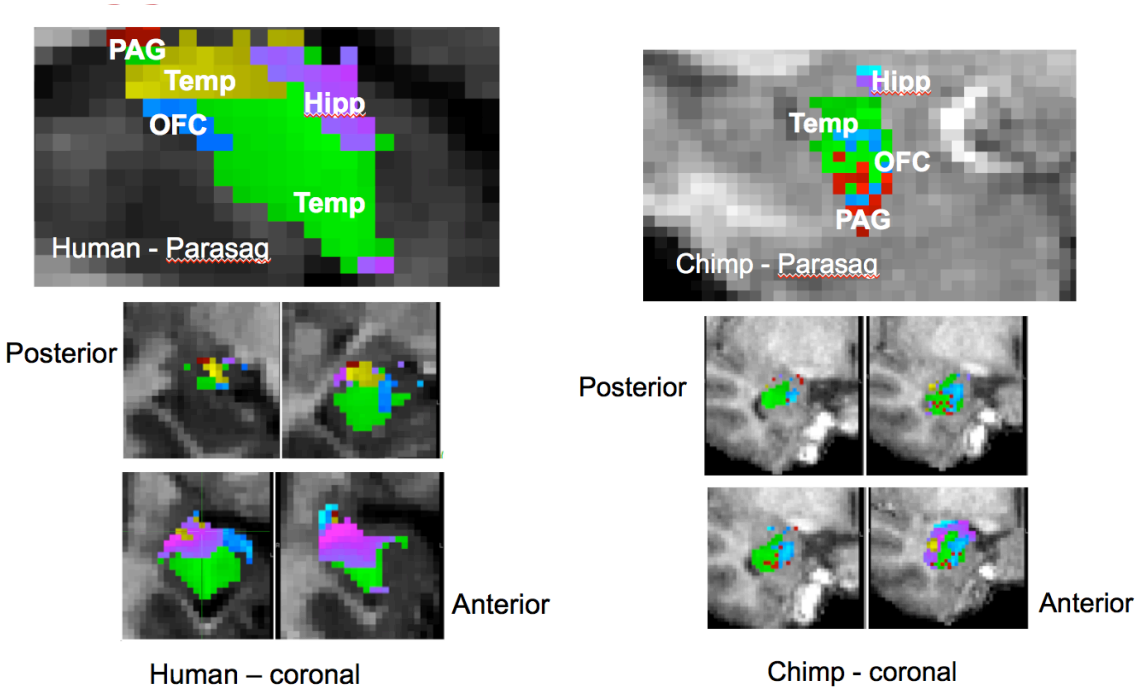

Figure 11 Find-the-biggest
A map of the highest probability voxels is shown for each of the regions of interest in the study in the human and chimp.

Find-the-biggest analysis.

The figures generated showed a maximum probability map for one representative chimpanzee and human that determine whether any seed target voxel has relatively stronger connections to the other target seed voxels in the amygdala mask. In this case, for each target voxel in the ROI mask drawing, the voxels in the amygdala mask in which it had stronger connections to was determined. It can be seen that the OFC had stronger connections to the ventral lateral portions of the amygdala, the PAG had stronger connections to the more

dorsolateral section of the amygdala and the olfactory cortex had stronger connections to the most dorsal medial cortical parts of the amygdala. This is consistent with previous histological studies (Sah et al., 2003).

Quantitative Results

As shown in Table 1, In the conservative amygdala analysis, the proportion of successful thresholded streamlines between the amygdala and primary olfactory cortex in the human cohort was significantly higher than the chimpanzee cohort (U=3.00, p<.05 (two-tailed), r=-.69); between the PAG-amygdala the difference was not significant between species (U=10.00, p>.05 (two-tailed)); for the temporal lobe-amygdala, the difference between the two species was not significant (U= 18, p>.05 (two-tailed)); for the hippocampus-amygdala, the difference between the two species was not significant (U=14, p>.05), and for the OFC-amygdala, the human data was significantly higher in humans than in chimps (U=2.00, p<.05 (two-tailed), r=.74).

Table 1. Proportion of streamlines for the conservatively-drawn amygdala tracts as a function of mask sizes

Species	Case	Mean	Median	STD
Chimp	PAG	0.000125599	0.000119358	3.01916E-05
Chimp	OFC	4.17691E-05	**3.86678E-05**	1.0577E-05
Chimp	Olfactory Cortex	0.000151502	**0.000141762**	8.68914E-05
Chimp	Temporal Lobe	1.98583E-05	1.92179E-05	4.09886E-06
Chimp	Hippocampus	0.000148669	0.000144375	2.2651E-05
Humans	PAG	0.000138403	0.000128972	3.41986E-05
Humans	OFC	8.9504E-05	**8.84046E-05**	3.6107E-05
Humans	Olfactory Cortex	0.000205707	**0.000218632**	7.33015E-05
Humans	Temporal Lobe	1.10383E-05	1.22964E-05	6.03779E-06
Humans	Hippocampus	0.000153383	0.0001698	4.82605E-05

As shown in table 2 for the liberal amygdala analysis, the proportion of successful thresholded streamlines between the amygdala and primary olfactory cortex in the human cohort was significantly higher than the chimpanzee cohort (U=3.00, p<05 (two-tailed), r=-.69); between the PAG-amygdala the difference was not significant between species (U=8.00, p>.05 (two-tailed)); for the temporal lobe-amygdala, the difference between the two species was not significant (U= 12, p>.05 (two-tailed)); for the hippocampus-amygdala, the differences were not significant (U=17, p>.05), and for the OFC-amygdala, the human data was not significantly different than the chimp data (U=6.00, p>.05 (two-tailed)).

Table 2. Proportion of streamlines for the liberally-drawn amygdala as a function of mask sizes

Species	Case	Mean	Median	STD
Chimp	PAG	9.82153E-05	9.95246E-05	2.80159E-05
Chimp	OFC	4.20948E-05	**4.12484E-05**	9.63416E-06
Chimp	Olfactory Cortex	0.000111241	**0.000108795**	1.84766E-05
Chimp	Temporal Lobe	2.14739E-05	2.10622E-05	4.31779E-06
Chimp	Hippocampus	0.000125754	0.000124899	1.27692E-05
Humans	PAG	0.000133823	0.00010877	5.21008E-05
Humans	OFC	7.90265E-05	**6.93767E-05**	3.00261E-05
Humans	Olfactory Cortex	0.000169765	**0.000192223**	4.98111E-05
Humans	Temporal Lobe	9.69839E-06	1.14223E-05	8.16302E-06
Humans	Hippocampus	0.000152019	0.000170811	4.65671E-05

A Mann-Whitney U analysis was also used to analyze the difference in the amount of overlap between the number of voxels (converted to volume) that contain thresholded tracts and the amygdala masks. This was done by dividing

the thresholded tract size by the volume of the amygdala for each tractography run in each species.

As seen in Table 3, in the conservative amygdala analysis, the proportion of successful thresholded tracts that intersected the amygdala to and from the primary olfactory cortex in the human cohort was significantly higher than the chimpanzee cohort ($U=0.00$, $p<.05$ (two-tailed), $r=-.83$); between the PAG-amygdala the difference was not significant between species ($U=7.00$, $p>.05$ (two-tailed)); between the hippocampus and amygdala, the overlap was significantly greater in humans than in chimpanzees ($U=12$, $p<.05$) and for the OFC-amygdala, the difference was not significant ($U=11.00$, $p>.05$ (two-tailed)).

Table 3. Proportion of the volume of the amygdala mask that contains thresholded tracts using the conservative amygdala masks of humans and chimpanzees.

Species	Case	Mean	Median	STD
Chimp	PAG	0.125880448	0.124420724	0.058978695
Chimp	OFC	0.27331311	0.212847311	0.163191764
Chimp	Olfactory Cortex	0.139202002	**0.129267276**	0.046537703
Chimp	Temporal Lobe	0.391017777	0.402648287	0.08307825
Chimp	Hippocampus	0.412715213	0.412132961	0.024116673
Humans	PAG	0.150251051	0.140980681	0.054310197
Humans	OFC	0.137744189	0.182093932	0.111015362
Humans	Olfactory Cortex	0.128134898	**0.127705044**	0.050145271
Humans	Temporal Lobe	0.465551962	0.493655762	0.273738789
Humans	Hippocampus	0.531510806	0.573117927	0.119695159

As shown in Table 4, in the liberal amygdala analysis, the proportion of successful thresholded tracts that intersected the amygdala to and from the primary olfactory cortex in the human cohort was not significantly higher than the chimpanzee cohort (U=16.00, p=.589 (two-tailed)); between the PAG-amygdala the difference was not significant between species (U=7.00, p=.93 (two-tailed)); between the hippocampus and amygdala, the humans was not significantly different (U=11, p>.05); between the OFC and the amygdala, the difference was not significant (U=18, p>.05); and between the temporal lobe and the amygdala, the difference between the two species was not significant (U=12, p>.05).

Table 4. Proportion of the volume of the amygdala mask that contains thresholded tracts using the liberal amygdala masks of humans and chimpanzees.

Species	Case	Mean	Median	STD
Chimp	PAG	0.078984376	0.074362165	0.054845864
Chimp	OFC	0.29930188	0.222256197	0.200049507
Chimp	Olfactory Cortex	0.044779636	**0.038347204**	0.033199033
Chimp	Temporal Lobe	0.399626676	0.43019744	0.080751378
Chimp	Hippocampus	0.511240506	0.53910007	0.106744503
Humans	PAG	0.130021215	0.128392578	0.025875166
Humans	OFC	0.209988555	0.193592063	0.037790717
Humans	Olfactory Cortex	0.148733832	**0.144838854**	0.0342959
Humans	Temporal Lobe	0.464421535	0.458935335	0.300380021
Humans	Hippocampus	0.576742961	0.607330677	0.124314581

4. Discussion

By conducting an in-depth analysis of the chimpanzee and human amygdala, using the connectivity patterns of the centromedial, basolateral and cortical amygdala, I generated a probability map of tracts to and from these regions as well as a probability map where these tracts intersect on the amygdala. Because there are so few chimp and human connectivity studies, most of the results were based on connectivity studies of the non-primate and macaque amygdalae. Nonetheless these connectivity profiles were used to select masks to provide information used to construct seed regions for analysis and tractographic reconstructions.

To the best of my knowledge, this is the first time that the connectivity of the major subdivisions of the amygdala has been systematically investigated in a comparative study of chimpanzees and humans with sizable cohorts. Other research methods used to study the nuclei of the amygdala include a cluster analysis of the connectivity of amygdala voxels with the rest of the gray matter (k-means clustering) (Solano-Castiella et al. 2010). However, with these methods what is missing is very much anatomical specificity - they have little to say about the specific connections of the amygdala and about what parts of the amygdala are connected with other brain regions. Thus, it's actually rather hard to relate to experimental studies of amygdala connectivity done in animals. My study is more relatable to those experimental studies. Furthermore, in my analysis, all target regions were specifically generated for the individuals' anatomy, and were also analyzed within the individual scan, instead of warping the ROIs and running

tractography in an averaged multi-subject template. The resulting amygdalar subdivisions from this analysis are therefore uniquely tailored to each individual's own anatomy, unlike many other human studies (Solano-Castiella et al. 2010).

It is important to note that this study was not without limitations. First, I was only able to analyze tracts that were as big as the largest voxel in the DTI, which may have prevented investigation of smaller tracts to and from the amygdala. In addition, volumetric differences in of the subdivisions of the amygdala between species could be due to either variation in the sizes of subdivisions or differences in connectivity strength between the two species. A possible future study could investigate this problem by applying this same method of DTI and probabilistic tractography to define the major regions of the amygdala in pathological patients with known lesions, and see how it affects the distribution. Although the small sample size (n=6 for each species) was chosen in order to preform a highly individualized analysis and the demographic data was comprised of a cohort of little variance in aspects such as age, future studies could further investigate the connectivity of the amygdalar subdivisions using a larger cohort with different populations. For example, our analysis came from the right amygdala of MRIs from a cohort from an aging study comprised of only adult females, and the method of analysis used in this paper could be useful in future investigations of the effects of aging on connectivity and amygdalar organization in a longitudinal study. It would be particularly interesting to investigate how the basolateral amygdala changes over time, based on the idea that the basolateral amygdala encodes valence to external stimuli, as Jacques

and colleagues found in a previous functional connectivity study that older adults experienced negative stimuli to be less negative than younger adults (Jacques et al, 2010). In addition it would be useful to obtain a larger cohort and investigate the subdivisions of the amygdala in male subjects that may be due to the effect that testosterone has on brain development (Filova et al., 2013). Another limitation is that DTI tractography does not control for tracts that run through but do not necessarily start or terminate in the amygdala target mask. This might lead to a higher waytotal result and obscure true organization patterns; however, this seems unlikely, because there aren't major tracts running through the amygdala.

In this study, I found that the basolateral amygdala was more strongly connected to the OFC in humans than in chimps in both the streamline-based analysis and the amygdala-overlap based analysis, both with high significance. This is an important finding that supports previous studies that have attributed human emotional specialization to expansion of the BLA and its reciprocal neural connections to neocortical regions like the OFC. The BLA-OFC connections have been thought to underlie many cognitive abilities, such as impulsive choice, learning and reversal learning, discrimination learning, expectation of outcome, and conditioned fear (Winstanley et al., 2004; Schoenbaum et al. 2000; Schoenbaum et al, 1999; Schoenbaum et al., 1998; Garcia et al., 1999). This increase in connective strength in the human lineage consistent with my results may be due to the evolutionary pressures of an expanding prefrontal cortex. Comparative studies of humans and apes have found that the prefrontal cortex is

larger relative to the rest of the brain, than in other apes. In addition, the region's supragranular layers are also larger in humans, providing more places for connections to occur, such as to and from the basolateral amygdala (Semendeferi et al., 2001). Furthermore, the social brain (or Machiavellian Intelligence) hypothesis, which argues that the cognitive demand of living in highly complex social groups selected for an expanded neocortex (Dunbar, 2003). Support for this hypothesis comes from studies that have found a positive correlation between social group size and basolateral volume complex (Emery et al., 2000), and the knowledge that this area has strong reciprocal connections to the neocortex. My findings, which suggest that humans have stronger connections between the basolateral amygdala and the OFC, support the social brain hypothesis and the assumption that this connection is likely to be involved in regulation of environmental cues with social significance and specialized cognitive demands for social tasks. In addition, lesioning of the BLA in rats has been found to result in social inhibition, which is a core characteristic of autism (Truitt et al., 2007). The BLA is also unique because it appears to be distinctly responsive to faces and actions of others in macaque studies (Brothers et al. 1990). My findings provide support that the BLA-OFC connection was selected for in human evolution as a means to enhance social intelligence, by providing valence to socially relevant stimuli like faces. My findings also suggest that autism may result from abnormalities in this connection.

It is also interesting to note the overlap data of the tracts from the OFC to the amygdala. Although the strength of the connection was significantly higher in

humans than in chimps using the streamline analysis, there was no significant difference in the proportion of the amygdala sending and receiving inputs to and from the OFC in chimps and humans. This suggests that human specialization may be accounted for not by the internal organization, specifically the proportion of the volume of the amygdala of the basolateral region, but rather the strength of its connections. In other words, this study suggests that humans may have more densely concentrated connectivity of the amygdala than do other primates, specifically chimpanzees. The qualitative overlap data are also consistent with Barger et al.'s study of the amygdaloid complex which found that human lateral nucleus of the basolateral division was larger than predicted in humans, and the basal nucleus of the basolateral division was larger than predicted in apes. The overlap results showed a more lateral preference for in the human subjects, and a stronger basal preference in the chimp amygdala results. The projections to and from the OFC subserve social cognition, providing further evidence that the basolateral region of the amygdala has been modified in human evolution due to social pressures (Barger et al, 2007).

This study also has implications for clinical psychiatric populations. This provides strong evidence for the claim that human specialization in the amygdala may have been localized to the basolateral amygdala. This is especially relevant when discussing emotional regulation and mood disorders. In a clinical study, researchers found that even in young children, high anxiety is associated with enlarged amygdala volume, specifically the basolateral amygdala (Qin et al., 2013). This can be interpreted as in part due to the BLA's interactions with

multiple brain systems, including the medial prefrontal emotion regulation system (Qin et al. 2013). Another study found that in patients with post-traumatic stress disorder (PTSD) the BLA complex had stronger functional connectivity with certain brain regions like the prefrontal cortex, which is implicated in cognitive control of emotional information which are the central explanations of the main symptoms of PTSD (Brown et al., 2014). With this evidence that emotional stress modifies the brain by strengthening the connectivity between the basolateral amygdala and medial prefrontal region, one can postulate that the because of the psychosocial stress present in human society, a evolutionary pressure has been put onto the BLA-OFC pathway to strengthen and counteract this anxiety.

Although I had initially hypothesized that the cortical amygdala would be more strongly connected to the primary olfactory cortex in chimpanzees than humans, the results have interesting implications. One study investing the anxiety and depressive behavior in rats due to early aversive life events found that the GABAergic cortical amygdala may be disrupted due to the effects of these traumas, causing depressive symptoms. However, the results also suggests that infant-conditioned odor, or odor cues associated with early life maltreatment, may function as a safety signal, by reducing depressive-like symptoms, and normalizing amygdala and piriform cortex activity in adulthood (Sevelinges et al., 2011). This suggests that stronger amygdala -to-olfactory pathway connections may have adaptive value that serves to normalize behavior and amygdalar activity, one that may have been selected for in humans with

complex emotional systems and social family constructs. This also suggests that odor processing may play a more significant role than previously thought in human emotion regulation.

5. References

Barger N, Stefanacci L, Schumann CM, Sherwood CC, Annese J, Allman JM, Buckwalter JA, Hof PR, Semendeferi K. (2012) Neuronal populations in the basolateral nuclei of the amygdala are differentially increased in humans compared with apes: A stereological study. Journal of Comparative Neurology. 520(13): 3035-3054

Barger N., Stefanacci, L., & Semendeferi, K. (2007). A comparative volumetric analysis of the amygdaloid complex and basolateral division in the human and ape brain. American journal of physical anthropology, 134(3), 392-403.

Baxter MG, Murray EA. (2002) The amygdala and reward. Nat Rev Neurosci. 3(7): 563-73

Brothers L., Ring B., Kling A., (1990), Responses of neurons in the macaque amygdala to complex social stimuli Behavioural Brain Research, 41, pp. 199–213

Brown VM, LaBar KS, Haswell CC, Gold AL; Mid-Atlantic MIRECC Workgroup, McCarthy G4, Morey RA5. (2014) Altered resting-state functional connectivity of basolateral and centromedial amygdala complexes in posttraumatic stress disorder. Neuropsychopharmacology. 39(2):351-9

Cirrarelli O, et al. (2006) Probabilistic diffusion tractography: a potential tool to assess the rate of disease progression in amyotrophic lateral sclerosis. Brain 129 (7) : 1859-1871

Dunbar R. (2003) The Social Brain: Mind, Language, and Society in Evolutionary Perspective. Annu. Rev. Anthropol. 32: 163-81.

Emery NJ, Perrett DI. (2000). How can studies of monkey brain help us understand 'theory of mind' and autism in humans? In Understanding Other Minds: Perspectives from Developmental Cognitive Neuroscience, ed. S Baron-Cohen, H Tager-Flusberg, DJ Cohen, pp. 274-305.

Filova A., Ostatn AD, Celec P., Hodosy J. (2013) The effect of testosterone on the formation of brain structures. 197(3):169-77.

Fischl, B., Salat, D.H., Busa, E., Albert, M., Dieterich, M., Haselgrove, C., van der Kouwe, A., Killiany, R., Kennedy, D., Klaveness, S., Montillo, A., Makris, N., Rosen, B., Dale, A.M., 2002. Whole brain segmentation: automated labeling of neuroanatomical structures in the human brain. Neuron 33, 341-355.

Fischl, B., Sereno, M.I., Dale, A.M., 1999. Cortical surface-based analysis. II: Inflation, flattening, and a surface-based coordinate system. Neuroimage 9, 195-207.

Fischl, B., van der Kouwe, A., Destrieux, C., Halgren, E., Segonne, F., Salat, D.H., Busa, E., Seidman, L.J., Goldstein, J., Kennedy, D., Caviness, V., Makris, N., Rosen, B., Dale, A.M., 2004. Automatically parcellating the human cerebral cortex. Cereb Cortex 14, 11-22.

Garcia, R., Vouimba, R. M., Baudry, M., & Thompson, R. F. (1999). The amygdala modulates prefrontal cortex activity relative to conditioned fear.Nature, 402(6759), 294-296.

Jacques, P. L. S., Dolcos, F., & Cabeza, R. (2009). Effects of Aging on Functional Connectivity of the Amygdala for Subsequent Memory of Negative Pictures A Network Analysis of Functional Magnetic Resonance Imaging Data. *Psychological Science*, *20*(1), 74-84.

Laberge F, Ahlenbrock-Lenter S, Grunwald W, Roth G. (2006) Evolution of the amygdala: new insights from studies in amphibians. Brain Behav Evol. 67(4):177-87

LeDoux JE, Iwata J, Cicchetti P, Reis DJ. (1988). Different projections of the central amygdaloid nucleus mediate autonomic and behavioral correlates of conditioned fear. J Neurosci 8(7):2517-29

Lehman, M.N., Winans, S.S., Powers, J.B., 1980. Medial nucleus of the amygdala

M. Jenkinson, C.F. Beckmann, T.E. Behrens, M.W. Woolrich, S.M. Smith. FSL. NeuroImage, 62:782-90, 2012

Murray EA (2007) The amygdala, reward and emotion. Trends Cogn Sci. 11(11):489-97

Pabba, M. (2013). Evolutionary development of the amygdaloid complex. *Frontiers in neuroanatomy*, *7*.

Qin S1, Young CB, Duan X, Chen T, Supekar K, Menon V. (2013) Amygdala Subregional Structure and Intrinsic Functional Connectivity Predicts Individual Differences in Anxiety During Early Childhood. Biol Psychiatry. pii: S0006-3223(13)00912-8

Reuter, M., Schmansky, N.J., Rosas, H.D., Fischl, B. 2012. Within-Subject Template Estimation for Unbiased Longitudinal Image Analysis. Neuroimage 61 (4), 1402-1418.

Sah, P., Faber, E. S. L., De Armentia, M. L., & Power, J. (2003). The amygdaloid complex: anatomy and physiology. Physiological reviews, 83(3), 803-834.

Schoenbaum, G., Chiba, A. A., & Gallagher, M. (1998). Orbitofrontal cortex and basolateral amygdala encode expected outcomes during learning. Nature neuroscience, 1(2), 155-159.

Schoenbaum, G., Chiba, A. A., & Gallagher, M. (2000). Changes in functional connectivity in orbitofrontal cortex and basolateral amygdala during learning and reversal training. The Journal of Neuroscience, 20(13), 5179-5189.

Schoenbaum, Geoffrey, Andrea A. Chiba, and Michela Gallagher. "Neural encoding in orbitofrontal cortex and basolateral amygdala during olfactory discrimination learning." The Journal of neuroscience 19.5 (1999): 1876-1884.

Semendeferi, K., Armstrong, E., Schleicher, A., Zilles, K., & Van Hoesen, G. W. (2001). Prefrontal cortex in humans and apes: a comparative study of area 10. American Journal of Physical Anthropology, 114(3), 224-241.

Sevelinges Y et al. (2011) Adult depression-like behavior, amygdala and olfactory cortex functions are restored by odor previously paired with shock during infant's sensitive period attachment learning. Developmental Cognitive Neuroscience. 1 (1): 77-87

Solano-Castriella et al. Diffusion tensor imaging segments the human amygdala in vivo. Neuroimage 49, 2958-2965.

Truitt, W. A., Sajdyk, T. J., Dietrich, A. D., Oberlin, B., McDougle, C. J., & Shekhar, A. (2007). From anxiety to autism: spectrum of abnormal social behaviors modeled by progressive disruption of inhibitory neuronal function in the basolateral amygdala in Wistar rats. Psychopharmacology, 191(1), 107-118.

Winstanley, C. A., Theobald, D. E., Cardinal, R. N., & Robbins, T. W. (2004). Contrasting roles of basolateral amygdala and orbitofrontal cortex in impulsive choice. The Journal of neuroscience, 24(20), 4718-4722.